

# Hyperspectral Imaging Technology for Pharmaceutical Analysis

Sara J. Hamilton and Robert A. Lodder

College of Pharmacy, A123 Advanced Science and Technology Center, University of Kentucky,  
Lexington, KY 40506-0286.

## ABSTRACT

The sensitivity and spatial resolution of hyperspectral imaging instruments are tested in this paper using pharmaceutical applications. The first experiment tested the hypothesis that a near-IR tunable diode-based remote sensing system is capable of monitoring degradation of hard gelatin capsules at a relatively long distance (0.5 kilometer). Spectra from the capsules were used to differentiate among capsules exposed to an atmosphere containing 150-ppb formaldehyde for 0, 2, 4, and 8 hrs. The second experiment tested the hypothesis that near-infrared (IR) imaging spectrometry of tablets permits the identification and composition of multiple individual tablets to be determined simultaneously. A near-IR camera was used to collect thousands of spectra simultaneously from a field of blister-packaged tablets. The number of tablets that a typical near-IR camera can currently analyze simultaneously was estimated to be approximately 1300. The bootstrap error-adjusted single-sample technique chemometric-imaging algorithm was used to draw probability-density contour plots that revealed tablet composition. The single-capsule analysis provides an indication of how far apart the sample and instrumentation can be and still maintain adequate S/N, while the multiple-sample imaging experiment gives an indication of how many samples can be analyzed simultaneously while maintaining an adequate S/N and pixel coverage on each sample.

## INTRODUCTION

Hyperspectral imaging is imaging of a target at a large number of discrete wavelengths. In its simplest form, a hyperspectral image forms a "data cube" in which two dimensions represent distances in space, while the third dimension represents spectral wavelength or wavenumber. Hyperspectral imaging is typically used in aerospace and defense applications, but applications in pharmaceutical analysis are also feasible<sup>1</sup>. Technology is available for spectrometric imaging at very long distances. The Predator remotely piloted reconnaissance aircraft is capable of hyperspectral imaging in the visible and infrared

regions<sup>2</sup>. The NASA Near Earth Asteroid Rendezvous (NEAR) spacecraft launched in 1996 began to orbit the asteroid Eros in 2000 at a distance of 200 km, and collected spectra from 804-2732 nm<sup>3</sup>. These spectra revealed that Eros is a moderately porous, chondritic asteroid with a composition similar to that of the protoplanetary disk. These successes suggest that a portable hyperspectral-imaging device might be useful in detecting contamination in the changeover between production of different pharmaceutical materials.

The perfect method for validation of cleaning would be capable of determining multiple chemical constituents and their locations simultaneously. The method would be quick and easy to use. Measurements made with the technique would be free of systematic bias and would be highly reproducible. The method would have good dynamic range and would be selective, so no characteristic of the environment would interfere with the measurement of any analyte. As the instrument approaches the ideal "analytical black box," it would be able to recognize that it is examining a sample unlike any it has ever examined before and would respond appropriately. This response could take the form of a request for operator assistance or for more samples of the same type, a "second opinion" analysis by another technique, or a library search for the best step to take. Hyperspectral imaging and chemometrics are increasingly approaching this ideal.

The purpose of this research was two-fold:

1. to provide an indication of how much distance can be between near-IR instrumentation and the sample while still maintaining adequate S/N in a single-capsule analysis, and
2. to provide an indication of how many samples can be analyzed simultaneously while maintaining an adequate S/N and pixel coverage on each tablet in a multiple-tablet analysis.

## Distance Study on Single Capsules

Gelatin capsules were selected as the model for the single-sample test. Gelatin is important to the pharmaceutical industry because of the diverse

formulations that can be incorporated into the hard gelatin capsule (HGC). Gelatin capsules are practical containers because of their strong but flexible backbone, polished appearance, capacity to hold dyes, and their solubility in aqueous solutions<sup>4</sup>. Gelatin is vulnerable to chemical modification, and formaldehyde modification of gelatin has been studied most extensively. Crosslinking of gelatin with formaldehyde has been used to manufacture enteric hard and soft capsules. Exposing gelatin capsules designed for immediate release of their contents to trace levels of formaldehyde may have an adverse effect on their *in vitro* dissolution rates. Contemporary research indicates that reduced *in vitro* dissolution rates, in contrast to decreased *in vivo* bioavailability of drugs, remain the chief consequence of crosslinking of HGCs with low levels of formaldehyde. For example, literature suggests that cornstarch, a common pharmaceutical excipient that sometimes incorporates a small amount of hexamethylenetetramine stabilizer, may form ammonia and formaldehyde upon hydrolysis.

The effect of lysine crosslinks on the dissolution of hard gelatin capsules containing amoxicillin is typically quantified 45 min after the capsules have been placed in a USP-standard dissolution apparatus. Exposure to 150-ppb formaldehyde gas drops the percent amoxicillin dissolved in such tests from 90% after no exposure to 20% after 8-hrs exposure to the formaldehyde. Previous literature indicates that these lysine crosslinks have signals in the near-IR spectral region from 5555 to 5880  $\text{cm}^{-1}$ <sup>4</sup>, so this spectral region was scanned in this experiment.

### Instrumentation

A 10-mW helium-neon (HeNe) laser (Spectraphysics, Eugene, OR) was used as a source of visible light for aligning the capsules and optics. The experiments were conducted outdoors to provide the unobstructed 500-meter path, and at night to simplify gross alignment of the optics using the visible laser. A 4-mW external cavity tunable diode laser (EOSI, Boulder, CO) was used as a source of near-IR light. Silicon CCD (Nikon) and indium antimonide (InSb)

cameras (Cincinnati Electronics, Mason, OH) were used during the alignment process. A Stanford Research Systems programmable waveform generator was used to modulate the near-IR light at 1 kHz. A small reflecting telescope with a 9-cm aperture was used to collect light for detection. A PbS telescopic detection unit<sup>5</sup> was temporarily removed from the one-meter near-IR telescope at the university to detect the modulated light from the capsules at 500 meters. A Dell PC and 16-bit A/D were employed for data collection. Digitized signals from the telescope preamplifier were cross-correlated with the signal from the programmable function generator, and Fourier transformed using GLIB software in Mathematica (Wolfram Research, Champaign, IL). To reduce the total data-collection time, signals were recorded at six different wavenumbers, 5797, 5764, 5731, 5682, 5634, and 5618  $\text{cm}^{-1}$ .

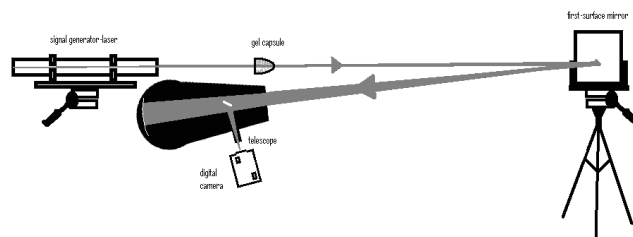


**Figure 1.** A schematic diagram showing the relationship of the instruments and optical path during collection of spectra at a distance of 0.5 km from a single gelatin capsule.

Precisely aligning the invisible near-IR laser following initial alignment with a visible laser would have been very difficult without interchangeable precision micrometer mounts. These mounts were constructed for this study in the machine shop of the Department of Physics and Astronomy. The physical length of the optical path was 250 meters. A 500-meter total optical path was achieved by reflecting the signal from the capsules at 250 meters backward using a 20-cm x 25 cm first-surface aluminized mirror (see Fig. 1). The distance from the laser to the capsule was two meters, although the beam spread was low enough to permit active excitation of the capsules with the laser at distances of up to approximately 200 meters.

## Results of Distance Study

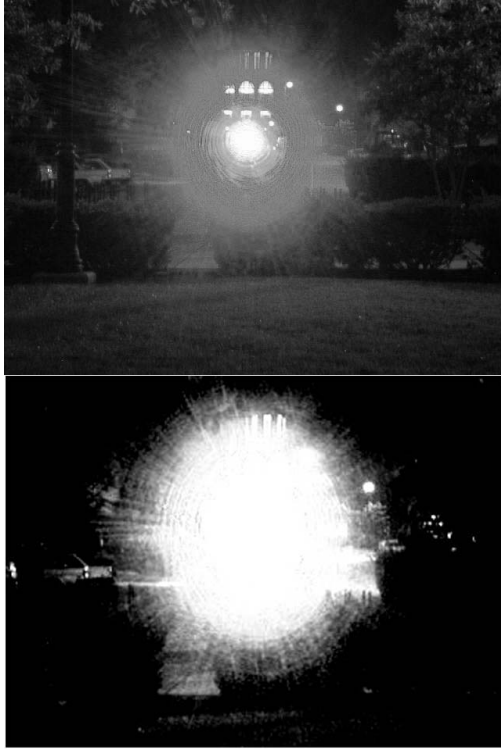


**Figure 2.** The visible light image (top) and near-IR light image (bottom) shows the intensity of the signal received over the 0.5-km path from a single gelatin capsule.

Fig. 2 shows the bright visible and near-IR images of the capsules on the 500-meter path. The intensity of the signals received suggests that spectrometry over even greater distances is possible. Spectra were collected individually from 24 hard gelatin capsules. Six of these capsules were not exposed to formaldehyde, while six were exposed to 150-ppb formaldehyde for two hours, another six for 4 hours, and the last six for 8 hours. Principal component regression of the spectra versus exposure time to formaldehyde produced  $r^2=0.89$ , with SEE = 1.17 hrs and SEP = 1.17 hrs. The calibration line is shown in Fig. 3.

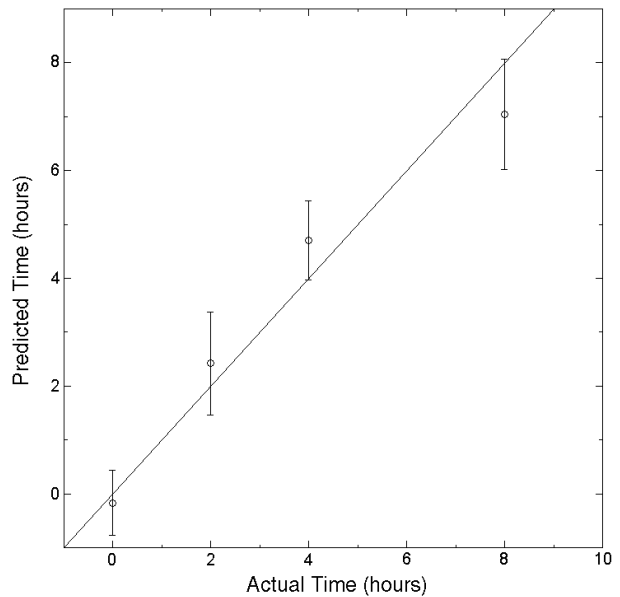


**Figure 3.** The actual vs. predicted exposure time to formaldehyde calculated using the spectra acquired at a distance of 0.5 km.

These results suggest that active-excitation spectrometry is a technique that is ripe for further research in pharmaceutical analysis. The active-excitation technique is particularly applicable to closed vessels where passive excitation does not reach. Indeed, NASA's Jet Propulsion Laboratory is working on a Multifunctional Active Excitation Spectral Analyzer (MAESA) for missions to planets like Pluto<sup>6</sup>. Pluto is so far from the sun that passive excitation would not be effective. The MAESA uses a laser to illuminate either a point or a line on a target. Raster scanning permits hyperspectral images to be collected. With the addition of a diffraction grating on the detection end of the system, active excitation can also be used to obtain Raman or fluorescence spectra. The NASA device features a wavelength response from 500-2500 nm, low power consumption, and a portable package design that operates near room temperature.

This single-capsule experiment suggests how far apart the sample and instrumentation might be while still maintaining adequate S/N. This experiment

suggests that remote sensing has applications in pharmaceutical analysis. For example, remote-sensing technology might some day be profitably applied to detection of small amounts of materials in a manufacturing environment.

The next step is to conduct experiments designed to detect protein contamination of clean glass and metal surfaces by scattering of light. These studies are just beginning. Tests will be conducted with a wavelength selection device (e.g., tunable filter) in front of a camera, and with a MAESA approach. Positive results would support the use of hyperspectral imaging and remote sensing to validation of cleaning in GMP processes.

### Number Study on Packaged Tablets

Aspirin was selected for study because its breakdown mechanism is well understood. Aspirin tablets can be placed in a blister pack so that breakdown can be initiated easily by placing a small hole in the package and putting the package into a hydrator. Thousands of aspirin tablets can be inexpensively packaged for hyperspectral imaging using a near-IR camera.

Near-IR cameras are also being employed increasingly in hyperspectral imaging experiments. Imaging spectrometers based on array cameras have fast scanning ability and high sensitivity. This study tests the hypothesis that a near-IR camera and hyperspectral imaging permits the identity and composition of large numbers of tablets to be determined simultaneously through blister packs to monitor drug stability.

### Materials

Near-IR images were obtained from 325-mg aspirin tablets (Kroger, Cincinnati, OH). Reference spectra were obtained from blister packaging (AH Robins, Richmond, VA), water, an aspirin tablet, and salicylic acid (Sigma, St Louis, MO). Aluminum foil backing (Reynolds, Richmond, VA) and cement (DAP, Dayton, OH) were used for sealing the polyvinyl chloride (PVC) blister packaging. Tetrabutyl ammonium phosphate (Eastman Kodak, Rochester, NY), monosodium phosphate monohydrate (Fisher, Pittsburgh, PA), ammonium hydroxide (Fisher), and methanol were used for the reference high-performance

liquid chromatography (HPLC) analysis of salicylic acid in aspirin.

### Instrumentation

An IRC-160 InSb focal plane array video camera (Cincinnati Electronics, Mason, OH) with near-IR bandpass cold filter was used for 0.5 m hyperspectral imaging of the samples. The camera frame rate was 51.44 frames/s and the photon energy response was 1800-10,000  $\text{cm}^{-1}$ . A polarizing filter for the camera reduced specular reflectance (Polaroid, Cambridge, MA). A tunable interference filter unit (OCLI, Santa Rosa, CA)<sup>7</sup> with photon energy response from 4325 to 5960  $\text{cm}^{-1}$  was mounted on the camera. A Mitsubishi IR-M300 PtSi 256 X 256 CCD array camera (Cypress, CA USA) was used at 2 m on the samples. The light source was 2 250W PC37771 near-IR/IR lamps (General Electric, Cleveland, OH). A monochromator system employing a concave holographic grating (American Holographic, Fitchburg, MA) and lead sulfide (PbS) detector was used for reference spectra<sup>7</sup>.

Whenever a near-IR camera was used to collect spectra, two spherical silicon dioxide reflectance standards (1 high reflectance, 1 low reflectance) were placed in each image to control for variations in light intensity and direction. Images collected on different days and with the light sources in different locations were made comparable by adjusting the gain and offset by multiplicative scatter correction<sup>8</sup> on the images so the intensities on the standards were identical. The specular reflectance on the standards was used to pin down the locations of the light sources and to supply a method to calibrate reflected specular light intensity. Diffuse reflectance from the rounded surfaces of the two standards was used to calibrate shaded areas and oblique surfaces in the images<sup>9</sup>. Two light sources were employed for spectrometric imaging to diminish shadows and attain the greatest signal-to-noise ratio (S/N) possible. The light sources were positioned at 90 degrees relative to one another, with the tablets at the vertex. The camera was placed between the light sources, at an angle of 45 degrees to each. Spectral images were obtained at each wavenumber with the near-IR light sources turned off, and again with them turned on, to correct for the existence of other lights in the room and for blackbody photon emission from the sample.

A hydrator was assembled to control the conditions under which the tablets decomposed<sup>1</sup>. Tablets in blister packages were exposed to water

vapor or a pH 9.0 ammonium hydroxide solution by punching a hole using a center punch through the foil support. Water absorption was determined by weighing and by near-IR spectrometry. The HPLC for analysis of salicylic acid used a C-18 column (Analytical Sciences, Santa Clara, CA), a Prostar 320 absorbance detector (Varian, Palo Alto, CA), a model 215 pump (Varian). The software for the near-IR equipment as well as the chromatography interface was written in C++ (Microsoft, Redmond, WA) and Speakeasy (Speakeasy Computing Corp, Chicago, IL). The mobile phase was 27:73 methanol:water, 0.15 M  $\text{NaH}_2\text{PO}_4$ , 5 mM tetrabutylammonium phosphate, at pH 6.0. This pH was selected to make the results comparable with our earlier study<sup>1</sup>. The half-life of aspirin at pH 6.0 is more than 5 days. Retention times for aspirin were approximately 5 minutes.

The tablet masses were measured with an electronic balance. Tablets were dissolved for HPLC analysis. A total of 43 tablets were selected from 172 hydrator tablets by principal component analysis (PCA) selection algorithm<sup>10</sup>. The benefit of this methodology is that it selects the best tablets to use in the calibration based on their near-IR spectra before reference measurements are obtained. The near-IR technique is fast and easy compared to the HPLC assay, making the selection of the optimum subset of tablets for the reference assay based on near-IR spectra valuable. The 172 tablets in turn came from four batches of 43 tablets, each sequence run for up to 24 hours in the hydrator<sup>1</sup>. By staggering the starting times of each 24-hour cycle it was possible to get at least six tablets in each hour of exposure from 0 to 24 hours. The four runs were made over a interval of two weeks.

### Imaging with the Bootstrap Error-adjusted Single-sample Technique (BEST)

The BEST method was employed to depict probability density contours for images at various distances in multidimensional asymmetric standard deviations (SDs)<sup>9</sup>. In the BEST, a population  $\mathbf{P}$  in a hyperspace  $\mathbf{R}$  represents the universe of possible spectrometric samples (the rows of  $\mathbf{P}$  are the individual

samples, whereas the columns are the independent information vectors, such as wavelengths or energies).  $\mathbf{P}^*$  is a discrete realization of  $\mathbf{P}$  based on a calibration set  $\mathbf{T}$ , which has the same dimensions as  $\mathbf{P}^*$  and is chosen only once from  $\mathbf{P}$  to represent as nearly as possible all the variations present in  $\mathbf{P}$ .  $\mathbf{P}^*$  has parameters  $\mathbf{B}$  and  $\mathbf{C}$ , where  $\mathbf{C} = E(\mathbf{P})$  and  $\mathbf{B}$  is the Monte Carlo approximation to the bootstrap distribution. The expectation value,  $E(\ )$ , of  $\mathbf{P}$  is the center of  $\mathbf{P}$ , and  $\mathbf{C}$  is a row vector with as many elements as there are columns in  $\mathbf{P}$ . Each new sample spectrum  $\mathbf{X}$  is projected into the hyperspace containing  $\mathbf{B}$  and many-one mapping the rows of  $\mathbf{B}$  onto the vector connecting  $\mathbf{C}$  and  $\mathbf{X}$ .  $\mathbf{X}$  and  $\mathbf{C}$  have identical dimensions. The integral over the hyperspace  $\mathbf{R}$  is calculated from the center of  $\mathbf{P}$  outward in all directions. The calculation of a skew-adjusted SD is based on a comparison of the expectation value  $\mathbf{C}=E(\mathbf{P})$  and  $\mathbf{C}=\text{med}(\mathbf{T})$ , the median of  $\mathbf{T}$  in hyperspace (with the same dimensions as  $\mathbf{C}$ ) projected on the hyperline connecting  $\mathbf{C}$  and  $\mathbf{X}$ . The result of the projection is an asymmetric SD that provides two measures of the standard deviation along the hyperline connecting  $\mathbf{C}$  and  $\mathbf{X}$ . Equation 1 defines the SD in the direction of  $\mathbf{X}$  in hyperspace, and equation 2 defines the SD in the opposite direction along the hyperline connecting  $\mathbf{C}$  and  $\mathbf{X}$ . Skew adjusted SDs can be used to calculate mean distances between spectra of different samples.

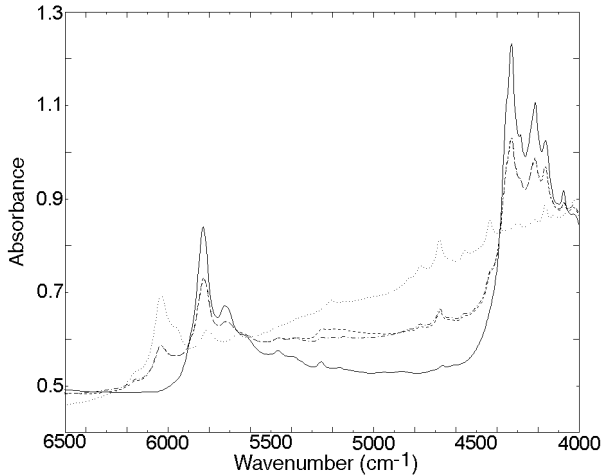
### Results and Discussion

Fig. 4 shows illustrative spectra of an aspirin tablet (dotted line), the blister package (solid line), an aspirin tablet in a blister package (dot-dashed line), and an aspirin tablet in a blister package with a leak exposing the tablet to moisture (dashed line). These spectra were obtained from single samples with the nonimaging spectrometer. The major peaks of the packaging are at  $5700$  to  $5800 \text{ cm}^{-1}$  and  $4000$  to  $4350 \text{ cm}^{-1}$ . The major spectral peaks of acetylsalicylic acid, at about  $6050 \text{ cm}^{-1}$  and  $4200$  to  $4800 \text{ cm}^{-1}$ , are apparent through the packaging. The most distinguishing spectral feature of salicylic acid arising through aspirin decomposition appears at  $6370 \text{ cm}^{-1}$ . The major water-absorbance peak appears at approximately  $5200 \text{ cm}^{-1}$ . This section of the spectrum contains only modest interference from the packaging, which simplifies the imaging of tablets. Calibration lines were computed for water and salicylic acid. The calibration lines were created using data obtained at 0.5 m from 43 tablets selected from 172 by the PCA method of Svensson et al.<sup>10</sup>. The spectra of the cross-

$$+\vec{\sigma} \left| \frac{\int_0^{+\sigma} (\int_{\mathbf{R}} \mathbf{P}^* \rightarrow \vec{CX})}{\int_{\mathbf{R}} \mathbf{P}^* \rightarrow \vec{CX}} = 0.34 \right. \quad (1)$$

$$-\vec{\sigma} \left| \frac{\int_0^{-\sigma} (\int_{\mathbf{R}} \mathbf{P}^* \rightarrow \vec{CX})}{\int_{\mathbf{R}} \mathbf{P}^* \rightarrow \vec{CX}} = 0.34 \right. \quad (2)$$

validation samples (by leave-one-out method) are overlaid on the calibration line. The standard error of estimate (SEE) for water was 0.05% of tablet mass and the SEP was 0.06% of tablet mass. For salicylic acid, the SEE = 0.06% of tablet mass and SEP = 0.06% of tablet mass.



**Figure 4.** Representative spectra of aspirin tablet (dotted line), the blister package (solid line), an aspirin tablet in a blister package (dot-dashed line), and an aspirin tablet in a blister package with a leak exposing the tablet to moisture (dashed line).

The PC (principal component) plot in Fig. 5 portrays water uptake by ten packaged tablets in the field of packaged tablets shown in the contour plot in

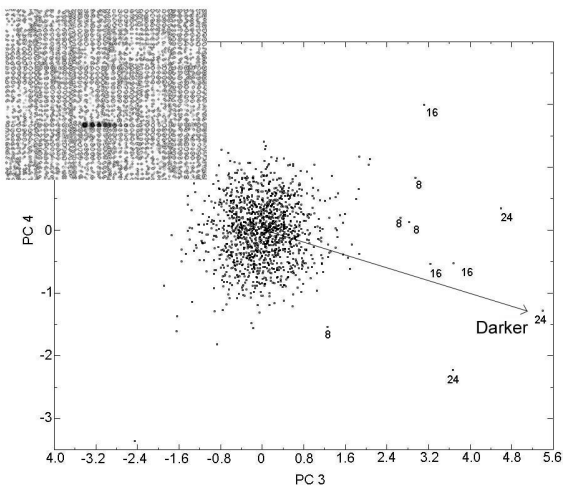


**Figure 5.** Contour plot with lines drawn in bootstrap error-adjusted single-sample technique standard deviations (SDs) for 10 packaged tablets in a field of 1286 packaged control tablets.

the inset. The tablets were imaged at 8, 16, and 24 hours after a hole was punched in the foil backing. The times are marked on each tablet in the plot. The endpoint was at the same time for all tablets, and the starting time (i.e., when the hole was punched) was varied. The tablet spectra were collected through the blister packaging, and the spectra are shown after multiplicative scatter correction. The spectra were used to calculate the contour plot in the inset of Fig. 5. The contours connect pixels with the same distance in multidimensional standard deviations (SDs) from the calibration tablets centered near the origin in the PC plot. The PC scores of the spectra show that the changing signal from water over time is readily detected through the blister packaging using a near-IR camera. In Fig. 5 a distance less than 3.8 SDs from the calibration set of normal tablets is displayed as light gray contour. A distance greater than 3.8 SDs in the direction of the spectrum of water (shown by the arrow) is colored progressively darker. The intensity of the black color is correlated to the magnitude of the distance in SDs between each pixel spectrum and the center of the spectra of control (dry) tablets. The maximum distance is 8.6 BEST SDs (corresponding to the tablet with the blackest density in the contour plot, and highest spectral peak at 5200 cm<sup>-1</sup>). Previous studies in nonpharmaceutical applications have suggested that there might be a minimum number of pixels required on a sample (e.g., 16) to achieve an acceptable S/N<sup>1</sup>. Part of the S/N problem with focal plane arrays arises from inactive ("dead") pixels and "flickering" pixels.

Some inactive pixels merely generate no output. However, inactive pixels often produce a stable signal beyond the typical range of values from normal pixels. The inactive pixel signal value does not change with a varying optical signal. Manufacturers commonly incorporate software corrections for these pixels into their equipment. These corrections automatically replace the signal values of the inactive pixels with the signal values of adjacent pixels. If a camera performs such an inactive-pixel correction automatically on booting without informing the operator, it can cause errors, especially when analyzing arrays of tablets in blister packaging. When a large number of tablets is in the field of view, only a few pixels are on each tablet; in these cases, it is easy for most or all of the values on an individual tablet to be inaccurate. If the correction software cannot be circumvented, one might never know that a tablet reading is essentially absurdity. For this reason, access to raw data from the camera (as used in this study) is preferred over corrected data.

Flickering pixels have a signal that varies randomly and partially independently of the actual optical signal. This characteristic makes flickering pixels much harder to correct reliably with automatic routines in actual camera use, because the varying signal could be real. In addition, if the system averages frames to generate a final image, then elementary averaging can obscure the flickering. Flickering pixels are usually not corrected in camera software. Imaging reference cards or scenes (in which the pixel output variation is known) at the beginning of camera operation will detect these pixels early, however. It is notable that flickering pixels frequently become inactive pixels with time. Approximately 0.1% of pixels in an InSb focal plane array (FPA) are ordinarily inactive or flickering, but this number grows slowly with thermal cycling and age of the focal plane array.

Figure 5 suggests that upper limit on the number of tablets that can be imaged concurrently on a 256 X 256 array is approximately 1300. With 1296 tablets in the camera field of view, at least 16 pixels can be applied in simultaneous sampling of each tablet, which is enough spectra on each tablet to get an effective S/N and form contours for imaging. Principal component analysis of the tablet spectra showed loadings with spectral features that correspond to salicylic acid and acetylsalicylic acid<sup>1</sup>.

## CONCLUSIONS

Hyperspectral imaging presents a potential speed improvement of approximately 30,000 over HPLC when analyzing moisture and salicylic acid in single, packaged aspirin tablets. Although the bulk imaging method is not quite as precise as spectrometric analysis of single tablets, the precision is close<sup>1</sup>. Hyperspectral imaging of a field of tablets is approximately 1000 times more rapid than spectrometry of single tablets. A near-IR camera including BEST image-analysis software permits multiple tablets to be analyzed simultaneously in blister packages. Further improvements in precision and sample throughput may come with

1. Positioning more pixels on the samples (e.g., using cameras with a higher detector density in the focal plane arrays),
2. Using several camera views and light-source positions at different angles to gather more diffuse reflectance, and
3. Increasing the integration time on the image.

Applications of conventional near-IR spectrometry are published almost every day in the pharmaceutical literature. Imaging and computing technology are changing many areas of scientific research. The next major advance of near-IR spectrometry in pharmaceutical analysis will likely come in the form of hyperspectral imaging, which enables immense numbers of samples to be analyzed simultaneously.

The single-capsule experiment suggests how far apart the sample and instrumentation might be while still maintaining adequate S/N. The multiple-tablet imaging experiment suggests how many samples can be analyzed simultaneously while maintaining an adequate S/N and pixel coverage on each sample. Together, these experiments suggest that hyperspectral imaging is capable of doing much more in pharmaceutical analysis than it is currently asked to do, and that this technology might some day be profitably applied to remote sensing of small amounts of materials in a production environment.

## ACKNOWLEDGEMENTS

The authors thank Mr. Mefford for constructing the precision mounts used in this project, and acknowledge the support of the National Science Foundation through CHE-9257998 and DGE-9870691.

## REFERENCES

1. Imran Malik, Mela Poonacha, Jennifer Moses, and Robert A. Lodder. "Multispectral Imaging of Tablets in Blister Packaging" *AAPS PharmSciTech*; 2 (2) article 9 (<http://www.pharmscitech.com>) 2001.
2. Naval Research Laboratory Press Release 60-00r, <http://www.pao.nrl.navy.mil/rel-00/60-00r.html>, October 31, 2000.
3. J. Veverka, M. Robinson, P. Thomas, S. Murchie, J. F. Bell III, N. Izenberg, C. Chapman, A. Harch, M. Bell, B. Carcich, A. Cheng, B. Clark, D. Domingue, D. Dunham, R. Farquhar, M. J. Gaffey, E. Hawkins, J. Joseph, R. Kirk, H. Li, P. Lucey, M. Malin, P. Martin, L. McFadden, W. J. Merline, J. K. Miller, W. M. Owen Jr., C. Peterson, L. Prockter, J. Warren, D. Wellnitz, B. G. Williams, and D. K. Yeomans, "NEAR at Eros: Imaging and Spectral Results", *Science*, 2088-2097, 22 Sept 2000.

4. T. B. Gold, R. G. Buice, Jr., R. A. Lodder and G. A. Digenis, "Determination Of Extent Of Formaldehyde-Induced Crosslinking in Hard Gelatin Capsules By Near-Infrared Spectrophotometry", *Pharm Res* 14(8), 1046-1050, 1997.
5. Colleen Scherer and Robert Lodder, "Using Natural Event Synchronizers With Near-Infrared Spectrometry In Remote Sensing," <http://www.spectroscopynow.com/>, 25 June 2001.
6. Q. Kim and NASA JPL, "a portable, near-room-temperature instrument would optically probe chemical compositions of surfaces," *Photonics Tech Briefs*, <http://www.ptbmagazine.com/>, Jan. 2002.
7. Ingle JD, Crouch SR. "Spectrochemical analysis." Prentice-Hall, Englewood Cliffs, NJ, 1988.
8. Isaksson T, Kowalski B. Piece-wise multiplicative scatter correction applied to near-infrared diffuse transmittance data from meat products. *Appl Spectrosc.*;47(6):702-709, 1993.
9. Dempsey RJ, Cassis LA, Davis DG, Lodder RA. Near infrared imaging and spectroscopy in stroke research: lipoprotein distributions and disease. *Ann NY Acad Sci.*;820:149-169, 1997.
10. Svensson O, Josefson M, Langkilde FW. Classification of chemically modified celluloses using a near-infrared spectrometer and soft independent modeling of class analogies. *Appl Spectrosc.*;51(12):1826-1835, 1997.